

Nonlinear refractive index measuring using a double-grating interferometer in pump–probe configuration and Fourier transform analysis

This article has been downloaded from IOPscience. Please scroll down to see the full text article.

2012 J. Opt. 14 035203

(<http://iopscience.iop.org/2040-8986/14/3/035203>)

View [the table of contents for this issue](#), or go to the [journal homepage](#) for more

Download details:

IP Address: 85.185.211.121

The article was downloaded on 01/05/2012 at 15:01

Please note that [terms and conditions apply](#).

Nonlinear refractive index measuring using a double-grating interferometer in pump–probe configuration and Fourier transform analysis

Saifollah Rasouli^{1,2} and Mahnaz Ghorbani¹

¹ Department of Physics, Institute for Advanced Studies in Basic Sciences (IASBS), Gava Zang, PO Box 45195-1159, Zanjan 45137-66731, Iran

² Optics Research Center, Institute for Advanced Studies in Basic Sciences (IASBS), Gava Zang, PO Box 45195-1159, Zanjan 45137-66731, Iran

E-mail: rasouli@iasbs.ac.ir

Received 12 November 2011, accepted for publication 12 January 2012

Published 2 February 2012

Online at stacks.iop.org/JOpt/14/035203

Abstract

In this paper, we have presented a simple, stable, highly sensitive and timesaving method based on a double-grating interferometer in conjunction with a pump–probe technique for measuring the nonlinear refractive index. A pump laser beam is aligned collinearly with an expanded plane parallel probe beam by a dichroic mirror. These beams pass through the sample, while right behind the sample using a suitable bandpass filter the pump beam is intercepted. The distorted probe beam then passes through a double-grating interferometer. One of the lateral shearing interference patterns is recorded by use of a CCD camera and, after digitization, has been stored in a computer. The interference pattern is analyzed by means of a Fourier transform algorithm. The refractive index changes have been obtained from phase distribution of the recorded fringe patterns. The implementation of the technique is straightforward and the arrangement is very simple and stable yet its sensitivity is comparable with other interferometry methods. It is also not a time consuming method. The method is applied for measuring the thermal nonlinear refractive index n_2 of colloidal gold nanoparticles in water solution.

Keywords: nonlinear optics, interferometry, gratings, phase retrieval, Fourier optics

(Some figures may appear in colour only in the online journal)

1. Introduction

The nonlinear refractive index is an important characteristic parameter of materials. Therefore, numerous techniques have been introduced for measuring nonlinear refraction in materials. Nonlinear interferometry [1–3], degenerate four-wave mixing [4], nearly degenerate three-wave mixing [5], ellipse rotation [6], beam-distortion measurements [7], Z-scan method [8, 9], the Z-scan based moiré deflectometry methods [10–12] and the non-scanning moiré deflectometry method in pump–probe configuration [13] are among the

techniques frequently reported. The first three methods, interferometry and wave mixing, are potentially sensitive techniques but require a complex experimental apparatus. Beam-distortion measurements, on the other hand, require precise beam scans followed by detailed wave-propagation analysis. The moiré-based methods are not very sensitive. The Z-scan technique [8, 9] is one of the convenient methods for the measurement of the nonlinear refractive index. But it has the disadvantage of being sensitive to the beam pointing instability and is sensitive to the power fluctuations. It is also a time-consuming method. Based on the principles of a

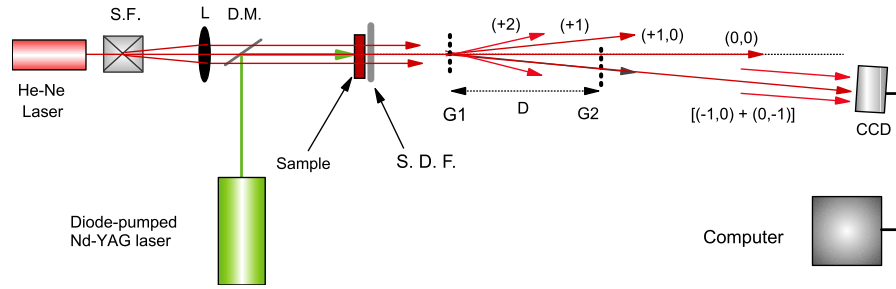


Figure 1. Schematic diagram of the experimental set-up. SF: spatial filter; L: collimating lens; DM: dichroic mirror; SDF: selective density filter; G1, G2: first and second grating, respectively. D stands for the distance between the two gratings.

double-grating interferometer in pump–probe configuration, however, we present a technique for measuring the refractive nonlinearities that offers simplicity and stability as well as high sensitivity. It is also not a time-consuming method. The technique is based on the transformation of phase distortion to deformation of the interference pattern of diffracted orders of a collimated beam when a pump beam propagates through the sample. Our arrangement is very stable. The method is a potentially sensitive technique yet does not require a complex experimental set-up. We demonstrate this technique on several materials in measuring the thermal nonlinear refractive index n_2 .

In this work a pump laser beam is aligned collinearly with an expanded plane parallel probe beam by a dichroic mirror. These beams pass through the sample, while right behind the sample using a suitable bandpass filter or an another dichroic mirror, the pump beam is intercepted. The distorted probe beam then passes through a double-grating interferometer. One of the lateral shearing interference patterns is recorded by use of a CCD camera and, after digitization, has been stored in a computer.

Fourier transform and phase-shifting methods are the basic techniques for phase retrieval of the sinusoidal fringe pattern in optical metrology [14–16]. In the traditional phase-shifting method it is needed to have at least three phase-shifted fringe patterns. The largest limitation of the phase-shifting interferometry for optical metrology is the sensitivity to the environment, both vibration and air turbulence. However, some novel dynamic phase-shifting methods are introduced to overcome these limitations [17, 18]. Implementation of these dynamic phase-shifting methods is not straightforward. Meanwhile, for one- and two-dimensional sinusoidal interference fringe patterns, the Fourier transform method is a well-known and straightforward method. In this work, the interference pattern is analyzed by means of a Fourier transform algorithm.

It should be mentioned that, while at first sight the technique employed here looks like a variant of the moiré method that we used previously, it is in fact an interferometric approach. In this work, unlike other interferometry methods for measuring phase distributions induced by a phase object [19], instead of separating the reference path and the probe path spatially we generate these two beam paths with the same optical elements for both beams. This feature and the small distance between the gratings provide a high stability set-up.

2. Theory

The schematic diagram of the experimental set-up shown in figure 1 is very simple. G1 and G2 are two identical gratings that are illuminated perpendicularly with an expanded monochromatic parallel beam, the probe beam. We define two coordinate systems, one for the incoming beams and the gratings (x', y', z') , and the other one for the interfering diffraction orders and the interference pattern (x, y, z) , figures 2(a) and (b). The gratings are set a distance D apart and their ruling directions make small angles $\theta/2$ and $-\theta/2$ by the x' axis. The z' axis shows the optical axis of the set-up, figure 2(a).

In order to avoid the overlapping of different diffraction orders, the distance between grating G2 and the observation plane should be larger than $\frac{Fd}{\lambda}$, where λ is the wavelength, d is the grating period and F is the aperture of the collimated beam. The incident plane probe wave before G1 will be distorted in the area of the pump beam propagating through the sample. Accordingly, the phase shift induced on the probe by the pump occurs only along its central region, whereas the outer region remains unaffected, figures 2(a) and (b).

The two laterally displaced interfering beams are the result of two subsequent negative first-order and zero-order (and vice versa) diffractions by the two gratings: one beam through the sequence: zero order \rightarrow negative first order, $u_{(0,-1)}$, and the other through the sequence: negative first order \rightarrow zero order, $u_{(-1,0)}$. Thus the beams are almost parallel together after passing through the two gratings and contribute to the final image, figure 2(a). A diaphragm behind the interferometer intercepts all other diffraction combinations. We chose a lateral shear larger than the size of the distorted area on the probe wavefront. In the distorted interference pattern the two laterally displaced interfering beams are overlapped in which one of them remains an unaffected plane beam and another one is the distorted carrier beam, figure 2(b).

In the theoretical considerations we assume that, before the pump beam illumination, the interfering orders of the probe beam are

$$\begin{aligned} u_{(-1,0)}(x, y) &= A_1 \exp(i\vec{k}_1 \cdot \vec{r}), \\ u_{(0,-1)}(x, y) &= A_2 \exp(i\vec{k}_2 \cdot \vec{r}), \end{aligned} \quad (1)$$

where A is the amplitude, \vec{k} is the propagation vector of the corresponding waves ($k = \frac{2\pi}{\lambda}$) and λ is the probe beam

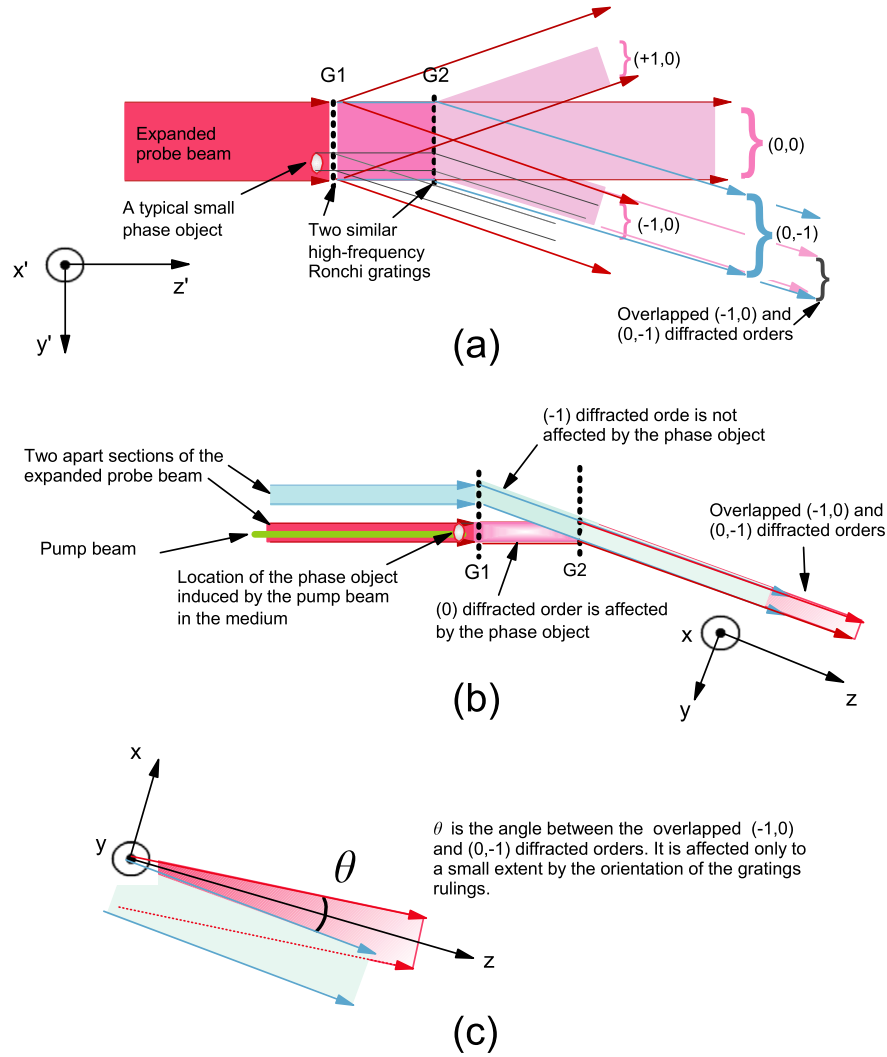


Figure 2. Schematic representation of the double-grating shearing interferometer in the phase object study, (a). Details of the overlapped diffracted orders, (b). Here the lateral shear is larger than the dimensions of the phase object. (c) The overlapped diffracted orders are shown, where the view point is rotated by 90°.

wavelength. Phase distribution of the interference pattern can be written as

$$\Phi_1 = (\vec{k}_1 - \vec{k}_2) \cdot \vec{r} = 2k \sin \theta x, \quad (2)$$

where θ is the angle between the two beams is affected only to a small extent by the orientation of the gratings rulings and x is the direction perpendicular to the interference fringes, figure 2(c).

After the pump illumination, its optical-field-induced refractive index changes in the nonlinear sample. The role of the electronic and thermal mechanisms in the process of refraction index changes in the interaction of intense laser light with matter has been studied in many papers [20–22]. Because the phase distribution of the distorted wavefront is actually the phase projection, the interfering fields can be written as

$$\begin{aligned} u'_{(-1,0)}(x, y) &= A_1 \exp(i\vec{k}_1 \cdot \vec{r}), \\ u'_{(0,-1)}(x, y) &= A_2 \exp(i\vec{k}_2 \cdot \vec{r} + \varphi(x, y)), \end{aligned} \quad (3)$$

where $\varphi(x, y)$ is the additional phase induced by the pump beam in the medium. Because the lateral shear is larger than

the radius of the pump beam, $u_{(-1,0)}(x, y)$ is not affected by the pump beam in the selected area of the interference pattern, figure 2(b). Now, in this case, the phase distribution of the interference pattern is

$$\Phi_2 = (\vec{k}_1 - \vec{k}_2) \cdot \vec{r} + \varphi(\rho) = 2k \sin \theta x + \varphi(\rho). \quad (4)$$

Now by subtracting equation (2) from (4) we have

$$\Delta\Phi(\rho) = \Phi_2 - \Phi_1 = \varphi(\rho). \quad (5)$$

The refractive index of the sample, n , which depends on the radiation intensity of the pump beam, may be expressed in terms of the nonlinear refractive index, n_2 , through $n(\rho) = n_0 + n_2 I'(\rho) = n_0 + \Delta n(\rho)$, where n_0 is the linear refractive index, $I'(\rho)$ is the irradiance of the pump laser beam within the sample, $\Delta n(\rho)$ is the light-induced refractive index change and ρ is the radial coordinate, $\rho = (x^2 + y^2)^{1/2}$. It should be mentioned that, in the measurement, total change on the refractive index of the test object (Au non-particles) and the suspension (water) is measured. It seems that the differences between the refractive index of the test object

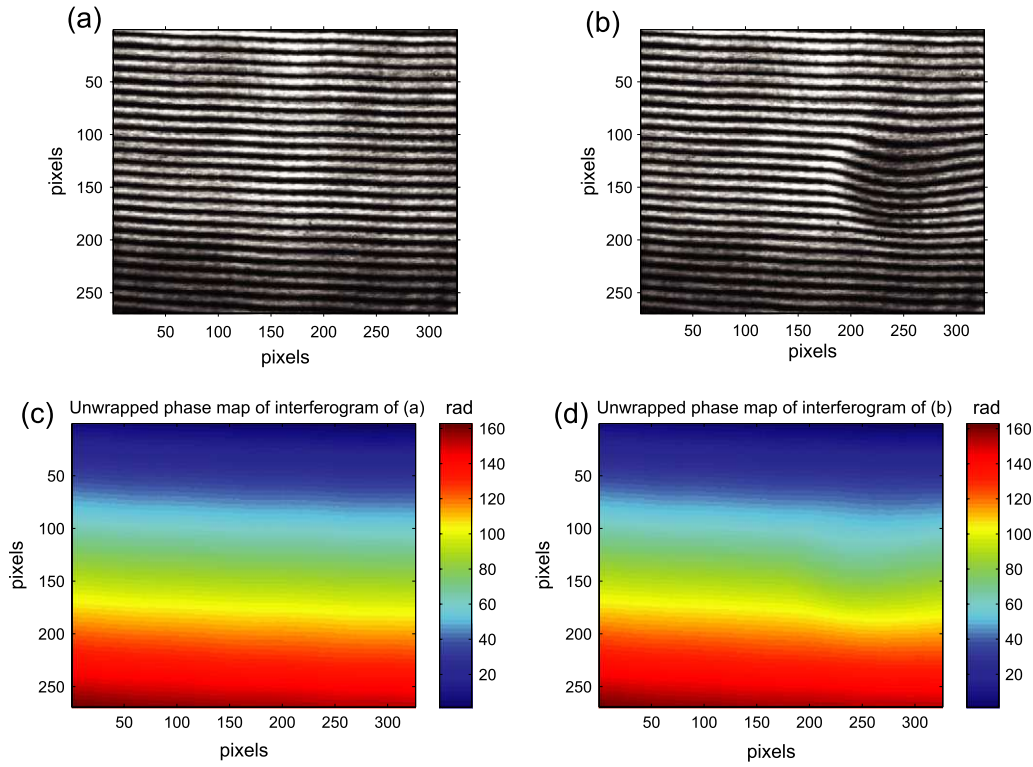


Figure 3. Typical shearing interferograms before (a) and after (b) the pump beam illumination. The corresponding unwrapped phase maps of the interferograms are shown in (c) and (d), respectively.

and the suspension can be affected in different ways for the thermal and electronic origins of the refractive index changes in the measurements. For a Gaussian pump beam traveling through the sample the radial dependence of the irradiance gives rise to a radially dependent refractive index change near the beam axis by

$$n(\rho) = n_0 + n_2 I'(\rho) = n_0 + n_2 \frac{2P'}{\pi w^2} \exp\left[-\frac{2\rho^2}{w^2}\right], \quad (6)$$

where P' is the total power of the pump beam and w is the pump beam radius. Now we can write the additional phase in the following form:

$$\begin{aligned} \varphi(\rho) &= n_0 k l + n_2 k l I'(\rho) \\ &= n_0 k l + n_2 k l \frac{2P'}{\pi w^2} \exp\left[-\frac{2\rho^2}{w^2}\right], \end{aligned} \quad (7)$$

where l is the thickness of the nonlinear medium and k is the propagation constant of the probe wave.

Finally, using equation (7) in equation (4), we have

$$\Delta\Phi(\rho) = n_0 k l + n_2 k l \frac{2P'}{\pi w^2} \exp\left[-\frac{2\rho^2}{w^2}\right]. \quad (8)$$

The phase of the interference patterns are analyzed by means of a Fourier transform algorithm and using equation (8) n_2 is determined.

3. Experimental details

We have examined the technique for measuring the thermal nonlinear refractive index n_2 in Au nanoparticles and Fe_2O_3

nanoparticles. In this paper, we refer to the measurements which were performed on 1 mM concentration of Au nanoparticles in water solution, with nanoparticle sizes of 5–7 nm, in a 4 mm thickness cell. Light from an He-Ne laser with wavelength $\lambda = 632.8$ nm with power 5 mW was first passed through a beam expander and a spatial filtering unit. A collimating lens of focal length 300 mm and diameter 42 mm was used to collimate the laser beam. The second harmonic of a 50 mW cw diode-pumped Nd:YAG laser beam at 532 nm is aligned collinearly with the collimated probe beam by a dichroic mirror. These beams pass through the sample. Right behind the sample using a suitable bandpass filter the pump beam is intercepted, and the probe beam strikes G1. The distance between the planes of G1 and G2 is chosen as 50 mm. Gratings G1 and G2 with a period of 1/100 mm were installed on suitable mounts. The holders of the gratings can be rotated around the optical axis to adjust the angle between the gratings. The sheared interferogram was recorded by a charge-coupled device CCD detector having 576 pixels \times 768 pixels with each pixel sized 13 μm \times 13 μm .

For calibration of the sign, the sample was replaced by a 100 μm thick glass slip and the fringe shift was recorded as the glass slip was rotated. The rotation of the glass slip introduced positive changes in phase and the corresponding direction of the fringe shift was noted as the calibration of the sign of phase change. The fringes for two different cases are shown in figures 3(a) and (b), when the pump beam was turned off and when it was turned on, respectively.

The recorded interferograms were processed using a fast Fourier transform algorithm. In the described experiment, a size of 269 pixels \times 326 pixels of the interferograms

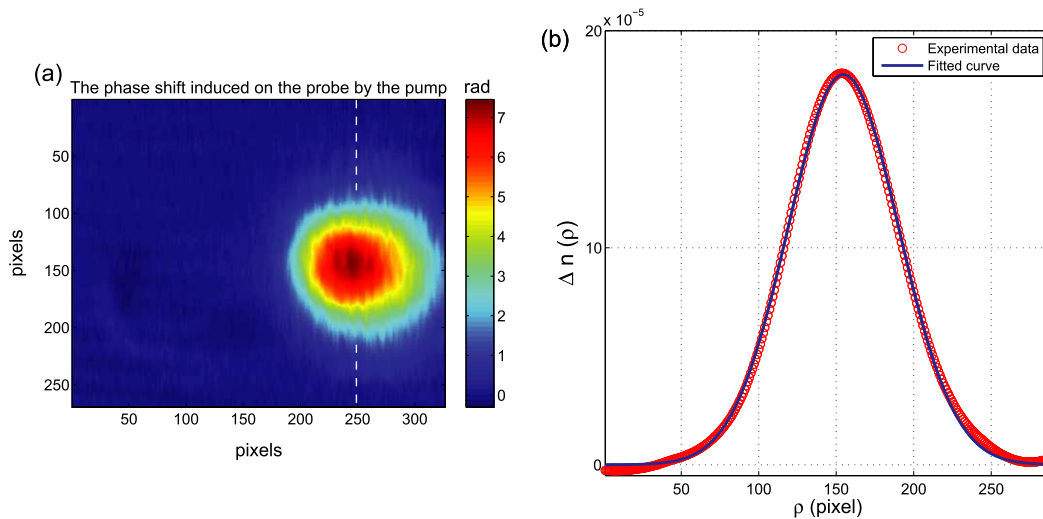


Figure 4. (a) The phase shift induced on the probe by the pump and (b) the measured induced refractive index profile $\Delta n(\rho) = n_2 I'(\rho)$ along the dashed line of (a).

was used to recover the phase maps. In figures 3(c) and (d) the corresponding unwrapped phase maps of the interferograms are shown, respectively. The phase shift induced on the probe by the pump is shown in figure 4(a). Figure 4(b) shows the plot of a profile of the induced refractive index along the dashed line of (a). The value of deviation of the experimental data from the theoretical model, $[(\Delta n_{\text{experimental}} - \Delta n_{\text{theoretical}})^2]^{1/2} \sim 2.5 \times 10^{-6}$, is obtained. For experimental values of $P' = 50$ mW and $w = 0.93$ mm, using equation (8), the mean value of n_2 obtained from a series of independent experiments is $-(4.8 \pm .1) \times 10^{-5} \text{ cm}^2 \text{ W}^{-1}$. This systematic error takes into account not only the fitting errors but also the reproducibility of the experiment. We have measured this quantity by the parallel moiré technique [12] and the results are compatible with each other. Unfortunately, in this paper we did not measure n_2 simultaneously by using the Z-scan technique³. But, there are comparable results for the nonlinear refraction index of Au nanoparticles which have been taken by using the Z-scan technique [22], if the difference in the concentration and filling factor of the composition of the colloidal particles is considered. The sensitivity of the method is comparable with other interferometry methods because it is, in fact, an interferometric approach.

4. Conclusion

In this paper, we have presented a new double-grating interferometer lay-out in conjunction with a pump-probe technique for measuring the nonlinear refractive index in materials. We have also used a Fourier transform algorithm for analyzing the interference pattern. The proposed method offers simplicity and stability as well as high sensitivity. The implementation of the technique is straightforward. In

³ Experimental comparison of our technique with the prevailing techniques such as Z-scan reported in the literature is the subject of future research at IASBS.

practice, by increasing the number of CCD pixels which is covered by a fringe spacing, one can increase the sensitivity of the method. Compared to the conventional methods, like the Z-scan method, this method is not a time-consuming method; rather it is quite fast. Also, the measurement is relatively insensitive to the alignment of the beams in the sensor and laser beam power fluctuation during the measurement. Finally, it seems that this method has an important practical application in measuring high power laser beam profiles.

Acknowledgments

The authors thank F Kabiri for useful help in sample preparation. Also, the authors acknowledge the anonymous referees for their constructive comments.

References

- [1] Weber M J, Milam D and Smith W L 1978 Nonlinear refractive index of glasses and crystals *Opt. Eng.* **17** 463–9
- [2] Moran M J, She C Y and Carman R L 1975 Interferometric measurements of nonlinear refractive-index coefficient relative to CS₂ in laser-system-related materials *IEEE J. Quantum Electron.* **QE-11** 259–63
- [3] Cotter D, Ironside C N, Ainslie B J and Girdlestone H P 1989 Picosecond pump-probe interferometric measurement of optical nonlinearity in semiconductor-doped fibers *Opt. Lett.* **14** 317–9
- [4] Friberg S R and Smith P W 1987 Nonlinear optical glasses for ultrafast optical switches *IEEE J. Quantum Electron.* **QE-23** 2089–94
- [5] Adair R, Chase L L and Payne S A 1987 Nonlinear refractive index measurement of glasses using three-wave frequency mixing *J. Opt. Soc. Am. B* **4** 875–81
- [6] Owyong A 1973 Ellipse rotations studies in laser host materials *IEEE J. Quantum Electron.* **QE-9** 1064–9
- [7] Williams W E, Soileau M J and Van Stryland E W 1984 Optical switching and n_2 measurements in CS₂ *Opt. Commun.* **50** 256–60

- [8] Sheik-bahae M, Said A A and Van Stryland E W 1989 High-sensitivity, single-beam n_2 measurements *Opt. Lett.* **14** 955–7
- [9] Sheik-bahae M, Said A A, Wei T, Hagan D J and VanStryland E W 1990 Sensitive measurement of optical nonlinearities using a single beam *IEEE J. Quantum Electron.* **26** 760–9
- [10] Jamshidi-Ghaleh K and Mansour N 2004 Nonlinear refraction measurements of materials using the moiré deflectometry *Opt. Commun.* **234** 419–25
- [11] Rasouli S and Jamshidi-Ghaleh K 2011 Erratum to ‘Nonlinear refraction measurements of materials using the moiré deflectometry’ *Opt. Commun.* **284** 1481–2
- [12] Rasouli S, Ghasemi H, Tavassoly M T and Khalesifard H R 2011 Application of ‘parallel’ moiré deflectometry and the single beam Z-scan technique in the measurement of the nonlinear refractive index *Appl. Opt.* **50** 2356–60
- [13] Rasouli S, Ghasemi H and Khalesifard H R 2008 Nonlinear refractive index measurement of the organic dyes using moiré technique and Talbot effect in pump-probe configuration *Proc. of 14th Annual Conf. on Optics and Photonics of Iran (In Persian)* pp 451–5
- [14] Fienup J R 1982 Phase retrieval algorithms: a comparison *Appl. Opt.* **21** 2758–69
- [15] Takeda M, Ina H and Kobayashi S 1982 Fourier-transform method of fringe-pattern analysis for computer-based topography and interferometry *J. Opt. Soc. Am.* **72** 156–60
- [16] Malacara D 2007 *Optical Shop Testing* (Hoboken, NJ: Wiley)
- [17] Wyant J C 2003 Dynamic interferometry *Opt. Photon. News* **14** 36–41
- [18] Toto-Arellano N I, Serrano-Garcia D I, Garcia A M, Zurita G R and Montes-Perez A 2011 4D profile of phase objects through the use of a simultaneous phase shifting quasi-common path interferometer *J. Opt.* **13** 115502
- [19] Xue L, Lai J, Wang S and Li Z 2011 Single-shot slightly-off-axis interferometry based Hilbert phase microscopy of red blood cells *Biomed. Opt. Express* **2** 987–95
- [20] Antipov O L, Bredikhin D V, Eremeykin O N, Savikin A P, Ivakin E V and Sukhadolau A V 2006 Electronic mechanism for refractive-index changes in intensively pumped Yb:YAG laser crystals *Opt. Lett.* **31** 763–5
- [21] Majles Ara M H, Javadi Z and Sirohi R S 2011 Measurement of nonlinear refractive index of Ag and Au nano-particles using moiré technique *Optik* **122** 1961–4
- [22] Souza R F, Alencar M A C, Silva E C da, Meneghetti M R and Hickmann J M 2008 Nonlinear optical properties of Au nanoparticles colloidal system: local and nonlocal responses *Appl. Phys. Lett.* **92** 201902